Environmental Radiation Studies Relevant to Thermoluminescence Dating

A. S. MURRAY, S. G. E. BOWMAN, and M. J. AITKEN
Research Laboratory for Archaeology, Oxford University, England

ABSTRACT

To determine the age of a potsherd by the thermoluminescence (TL) technique, one must have an accurate knowledge of the cosmic and environmental gamma dose rate in quartz. This is obtained by leaving a sensitive TL dosimeter, e.g., CaF_2 (MBLE type S), buried as near as possible to the position from which the sherd was removed. Quartz cannot be used directly because it is not sufficiently sensitive. The ratios of the response of a quartz-like dosimeter to those of CaF_2 and LiF, when the dosimeters are exposed to an infinite-matrix natural gamma spectrum, have been measured. This experiment used a 1-m cube of concrete containing 3000 ppm of uranium and its daughters. Smaller, less active matrixes of ^{40}K and thorium and its daughters have also been constructed. A means of making direct dose-rate determinations when the site context remains but burial of a dosimeter is impractical was developed using a NaI(Tl) system. It was possible to choose a threshold value (0.45 MeV) above which the number of gamma counts is directly proportional to the dose rate in CaF_2 irrespective of the relative concentrations of the natural emitters present. The equipment was field tested on ~40 Peruvian archaeological sites, and results are compared with CaF_2 measurements.

The basic notion of thermoluminescence (TL) dating of archaeological ceramics is expressed in the simplified age relation:

$$\text{Age} = \frac{\text{TL accumulated since firing by ancient man}}{(\text{TL/rad}) \times (\text{rads/year})}$$

The TL is carried by mineral inclusions in the clay fabric of the pottery (e.g., quartz and feldspar), and the radiation dose rate is provided by radioelements in the clay and in the surrounding burial soil. Cosmic radiation contributes a few percent also. It is convenient for discussion to take the following levels as typical:

Uranium, 2.8 ppm
Thorium, 10 ppm
K_2O, 2%

Obviously these levels vary widely depending on the geology of the region concerned. There is also a contribution of < 2% from rubidium, typically present at a level of 100 ppm (Warren, 1978).

Although for such levels the dose rate from alpha particles is 80% of the whole—with the external gamma dose rate from the soil amounting to only 7%—when account is taken of the much lower effectiveness of alpha particles in producing thermoluminescence (typically a factor of 7) (Zimmerman, 1972), the dominance by this type of radiation is removed. In terms of effective dose rates, the contributions are as follows:

Alpha, 40%
Beta, 36%
Gamma, 22%
Cosmic, 3%

The importance of the gamma contribution is further enhanced in the quartz-inclusion technique, which is one of the two main methods routinely used for TL dating today, the other being the fine-grain technique. In the inclusion technique quartz grains ~100 μm in diameter are extracted from the pottery, and the TL measurements are made on these. Because the average range of alpha particles from the uranium and thorium series is only 25 μm, the inner cores of such grains receive dosages only from beta and gamma radiation. Thus, if the outer layers of the grains are etched away with hydrofluoric acid, the alpha particle contribution can be reduced to negligible proportions. The effective dose rates, again for the typical levels of radioactivity, are then:

Beta, 206 mrads/year
Gamma, 125 mrads/year
Cosmic, 15 mrads/year

Thus gamma radiation contributes 36% of the whole, and the accuracy of the TL data obtained is highly dependent on its reliable evaluation. This greater dependence on environmental dose rate is of course a drawback. The quartz inclusion technique is, nevertheless, preferred because, unlike the fine-grain technique, it is not prone to the malign phenomena of anomalous fading (Wintle, 1973).

The breakdown of the gamma dose rate is given in Table 1 on the basis of data obtained by Bell (1976, 1977) by equating energy absorbed to energy released—the latter being derived from relevant nuclear data tables. The X-ray contribution is included in the gamma dose rate, but the internal conversion electron contribution is excluded.

Often the radioactivity of the pottery is different from that of the burial soil. To avoid sample material from the region in which the beta dose rate is transitional between the two levels, we discarded the outer 2-mm layer of each specimen. Because the thickness of the pottery fragment is not usually more than 20 mm, it is assumed that the internal contribution to the gamma dose rate is negligible and that the external contribution is not significantly attenuated.

TABLE 1

Gamma and X-Ray Dose Rates for an Infinite Medium of Soil*

^{238}U series	
Radioisotopes before ^{222}Rn	1.1
^{222}Rn and later	30.6
^{235}U series	0.5
^{232}Th series	
Radioisotopes before ^{220}Rn	20.8
^{220}Rn and later	30.6
^{40}K	41.0
Total	124.6

*The soil contains 2.8 ppm of uranium, 10 ppm of thorium, and 2% K_2O (in mrads/year). The principal gamma emissions above 1 MeV are 1.76 MeV from ^{214}Bi (post ^{222}Rn), 2.65 MeV from ^{208}Tl (post ^{220}Rn), and 1.46 MeV from ^{40}K; these carry 4, 15, and 33%, respectively, of the total gamma dose rate.

In the following sections we describe two methods currently used for on-site measurement of the environmental dose rate. In the first, a small capsule of highly sensitive TL dosimeter powder is buried in the same surroundings or in surroundings as similar as possible to those from which the pottery fragments were removed. In the second, a sodium iodide scintillator is used; its electronic threshold is chosen so that the conversion factor from count rate to dose rate is independent of whether the predominant radioisotope is uranium, thorium, or potassium. The first method is the preferred technique because the capsule can be inserted into position with less disturbance than can the scintillator. It also has the advantage that, site permitting, it can be left in position for a year to average out seasonal variations in water content (Mejdahl, 1970, 1972).

For sites on which it is not possible even to make scintillator measurements, radioactive analyses of soil samples are made in the laboratory. Currently this is done with a NaI gamma spectrometer, for which the minimum sample size is 100 g. An intrinsic germanium well-type detector with a sample size of 10 g is shortly to be commissioned. Thick-source alpha counting with a zinc sulfide screen, combined with flame photometry for potassium determination, is an alternative. The disadvantage of alpha counting is that an average thorium-to-uranium ratio must be assumed in deducing the gamma dose rate, and the ratio of gamma dose rate to alpha count rate differs strongly between the two series (it is higher by a factor of 1.5 in the thorium series). Another disadvantage of both methods of laboratory analysis is that for some soils there is substantial escape of radon and the degree of escape may be different when the sample is being counted in the laboratory from what it was when in the ground. The level of 21-year ^{210}Pb can be used to measure the in situ radon retention, however. At present this is measured by alpha spectrometry of deposited ^{210}Po, but with the germanium detector the 46-keV gamma emission from ^{210}Pb itself will be used. Besides radon escape, there are other forms of decay-chain disequilibriums that may upset laboratory evaluation, particularly the alpha counting method.

Whether on-site or laboratory measurements are used, a strong consideration in the selection of samples for TL dating is the homogeneity of the immediate surroundings (to a distance of 0.3 m). This is more acute in the case of laboratory measurement, but it is also a limitation of on-site measurements because of the practical difficulty of positioning even a small capsule so that it receives the same gamma flux as the pottery fragment removed for dating. Another factor to be considered is the rapidity with which the pottery became buried.

For an account of the other aspects of archaeological TL dating, see Aitken, Zimmerman, and Fleming (1968), Zimmerman (1971), Aitken and Fleming (1972), Aitken (1975), and Fleming (1977). Currently it is practical to think in terms of a dating uncertainty of 5 to 10% of the age. Thus it is reasonable to set an uncertainty of 5% as the objective for accuracy of assessment of the environmental dose rate.

SIMULATION OF SOIL SPECTRA

Whether we are considering the use of a thermoluminescence dosimeter or a scintillator to evaluate gamma dose rate in the ground, we are faced with the problem that, although the primary spectrum may be well-known, the secondary spectrum resulting from photon degradation through Compton interactions is not. Since a thermoluminescence dosimeter measures absorbed dose, knowledge of the spectrum is needed only to correct for any differences in mass absorption coefficients between dosimeter material and the relevant mineral in the pottery, i.e., quartz (SiO_2)—and perhaps for attenuation effects in the capsule wall. From Fig. 1, we see that, as

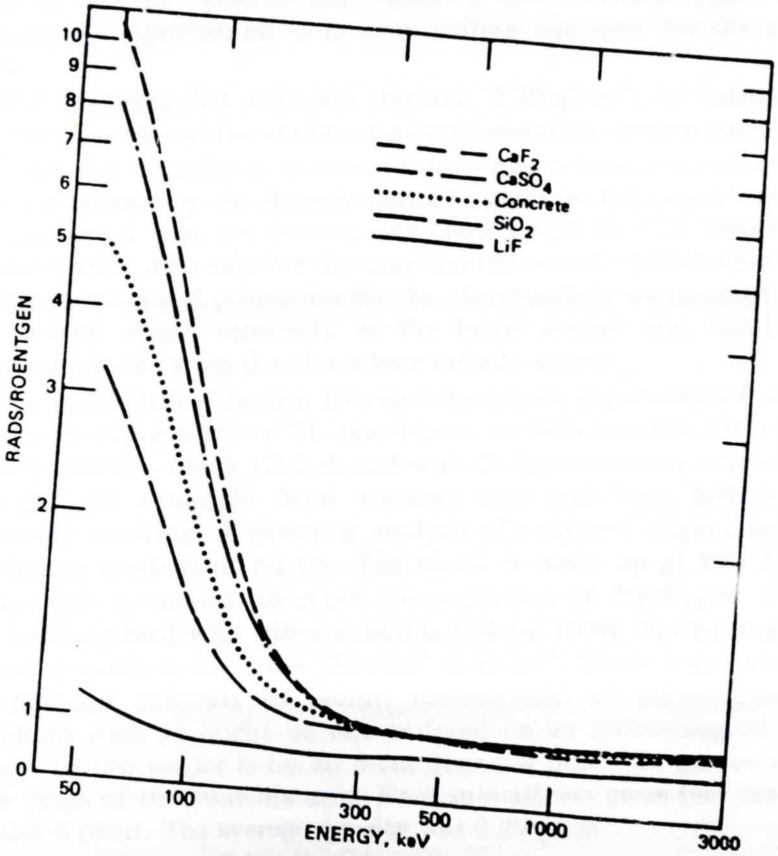

Fig. 1 Energy absorption characteristics of various materials, calculated from Storm and Israel (1970) and Evans (1968b): $(\mu/\rho) = \Sigma_i (\mu_i/\rho_i)w_i$, where μ_i/ρ_i is the mass absorption coefficient of the element concerned and w_i is the fraction by weight (Evans, 1968b).

long as the major part of the absorbed dose comes from photons above 0.2 MeV, the correction for differences in mass absorption coefficients is unlikely to be a strong one. On the other hand, the factor for converting scintillator count rate to soil dose rate depends strongly on the size of the scintillation crystal and its absorption characteristics and on the gamma spectrum being measured.

As an alternative to dealing with this problem by computation, we built three concrete blocks, 51 by 51 by 51 cm, one each doped with uranium, thorium, and potassium and each having a pluggable access channel to its center to permit insertion of a capsule or scintillator. A fourth undoped block of the same size was built as a background monitor. The uranium and thorium additives were chemically analyzed New Brunswick sands from the U. S. Department of Energy, pitchblende (sand 6) and monazite (sand 7A), respectively. Agricultural potassium sulfate was used for the third block.

For the expected concrete density, 2.35 g/cm^3, we calculated that the dose rate at the center of a block should be within 5% of the dose rate for an infinite matrix of the same radioactive concentration. Unfortunately the density turned out to be 1.93 g/cm^3, and it was calculated that the central dose rate would be ~7% below the infinite-matrix dose rate for the uranium block and ~11% below that for the thorium and potassium blocks. Nevertheless, we assumed that the spectral shape, especially at the lower energy end, would be indistinguishable from that for a true infinite matrix.

As an additional facility to make short-term experiments feasible with relatively insensitive TL phosphors, we later constructed a large (1 m^3) concrete block (U3) doped with 15 kg of uranium ore, which was part of a sample from Katanga that had been left in the university museum. A chemical analysis of unknown origin specified a uranium content of 53.1%. The block is made up of 125 20-cm cubes with a nominal uranium concentration of 3000 ppm. These can be assembled with other subunits (10 by 10 by 20 cm) to give a matrix variable in size from (20 cm)^3 to (1 m)^3. There is also a range of undoped subunits to permit investigation of inhomogeneous situations such as might be encountered on an archaeological site. Access to the center is by an 8-cm diameter hole that can be filled with plugs of the same material. Each subunit was given two coats of emulsion paint. The average density was 2.27 g/cm^3.

Table 2 gives the results of analyses of U3 components using a NaI(Tl) system calibrated against sealed concrete masters made from New Brunswick sands and potassium chloride. The large error limit in item 2 arises from uncertainty as to the amount of water added (and

TABLE 2

Apparent Uranium Concentrations in Block U3 Determined by Gamma Spectrometry*

Condition	Before sealing	After sealing	Implied radon escape
1. Ore concentration evaluated from γ measurement on accurately weighed mix into concrete	49.4%	53.6%	8%
2. Calculated concentration in U3 from item 1 and weights of ingredients		3010 ± 100 ppm	
3. U3 concentration according to samples abstracted from concrete mix	2625 ± 25 ppm	2835 ± 35 ppm	7.5%

*Radiochemical measurement of the ^{210}Po activity in the ore gave a value corresponding to 53 ± 3% that of the parent.

the exact water content at present). We took 2835 ± 35 ppm as the preferred value. Using data from Table 1 and an assumed figure of 4 ± 2% for the radon escape from the actual subunits, we predicted the dose rate at the center of U3 to be 31.4 ± 0.8 rads/year. Note that, although the data for the 1.76-MeV emission from ^{214}Bi is well-established, this is not the case for the myriad other emissions from ^{214}Bi. Table 1 is based on the findings of Bell (1977), which made a downward revision of 10% in this earlier value for the uranium series gamma energy release (Bell, 1976).

The characteristics of all blocks used are summarized in Table 3.

EVALUATION OF DOSE RATE BY THERMOLUMINESCENCE CAPSULE

The thermoluminescent powder used in this work was natural CaF_2 (Super S fluorite kindly supplied by Manufacture Belge de Lampes et de Material Electronique S/A, Brussels). This powder can be used down to dose levels of a fraction of a millirad if appropriate precautions are taken (Aitken, 1968). Unfortunately it is not available commercially. Its other disadvantages are that it has some sensitivity to light, particularly sunlight or fluorescent light and it has a significant self-dose, estimated at 11 mrads/year for Super S fluorite. A commercial alternative is $CaSO_4$ doped with dysprosium or thallium, which has an insignificant sensitivity to light. There are conflicting reports as to whether it exhibits fading, however; possibly

TABLE 3

Summary of Data for Radioactive Concrete Blocks

Characteristic	Block*			
	K	Th	U1	U3
1. Concentration† of parent	6.5% of K_2O	191 ppm (plus 7 ppm U)	170 ppm	2835 ppm
2. Calculated dose rate (assuming no gas loss), rads/year	0.133	1.02	1.97	32.7
3. Predicted loss from gas escape‡		0.04 ± 0.04	0.2 ± 0.05	1.3 ± 0.7
4. Measured dose rate§ after subtracting background, rads/year	0.12 ± 0.01	0.62 ± 0.03	1.22 ± 0.05	34.6 ± 1.5
5. Ratio of Item 4 to Item 2 − Item 3, with allowance for noninfinite size	1.03 ± 0.1	0.73 ± 0.07	0.78 ± 0.06	1.10 ± 0.05
6. Size (side of cube)	51 cm	51 cm	51 cm	1 m

*For K, Th, and U1, the measured dose rates are averages of all types of capsules used. For a discussion of the discrepancy between predicted and measured dose rates, see Bowman, 1976.

†Concentrations for Th and U1 are calculated from weights of ore (sands 7A and 6, respectively) and concrete constituents used. For K and U3 concentrations were determined by flame photometry and gamma spectrometry, respectively.

‡Loss from gas escape was estimated by gamma spectrometry of laboratory samples.

§Measured dose rate in the undoped 51-cm concrete block was 63 mrads/year; that in U3 was derived as described in text.

this depends on the method of preparation. For peak III of Super S fluorite, the fading measured over a 5-year period was equivalent to less than 1%/year.

In use, ~50 mg of powder are sealed in a capsule and buried in an auger hole at the relevant position on the site for a period upwards of several weeks. As mentioned earlier, the optimum burial time is a year but, as in the application described later in this paper, this is not always practical. The powder is drained of previous TL as late as possible before burial and is measured as soon as possible after retrieval. If the powder is carried in a lead container with 1-in. walls, the dose rate is typically about 0.1 mrad/day, but, in the application described here, circumstances permitted a container of only 0.25-in. wall thickness. Measurement consists of comparing the height of the TL glow peak (III) with that induced by subsequent irradiation with a laboratory ^{90}Sr–^{90}Y beta source calibrated against a ^{137}Cs gamma source standardized by the National Radiological Protection Board, Harwell (Wintle and Murray, 1977).

Initially aluminum-alloy capsules were used. These were chosen because the average atomic number of both soil and CaF_2 is close to that of aluminum. A significant alpha activity was found in all types of aluminum tested, however, even in super-pure aluminum. Next, capsules of black nylon with wall thicknesses of 4 mm to shield off beta particles were used. At present copper capsules with walls 0.7 mm thick, an internal diameter of 3 mm, and a length of 15 mm are being used. They are sealed by hard soldering and, hence, can be conveniently annealed (at 500°C) in a portable oven designed to run from an electric-light socket.

Now let us consider, first, the validity of using CaF_2 as a dosimeter for evaluating the dose rate to quartz and, second, the effect of different wall materials. The TL response of CaF_2 cannot be compared with that of quartz directly, even in the more active U3 block, because quartz is too insensitive.

As can be seen from Fig. 1, CaF_2 has a strong overresponse relative to quartz at low energies; at high energies the value of rads per roentgen drops to about 0.98 that of quartz. Hence the two materials have the same response to the gamma flux in the ground only if low-energy photons deposit an insignificant portion of the absorbed energy. The question of spectral distribution of energy flux was considered by Mejdahl (1970) with respect to the TL dosimeter material $CaSO_4$–Dy. He used polyethylene capsules in a 1.5-mm-thick steel tube. Besides being convenient for driving the dosimeter into the ground, the steel modifies the incident spectrum so that the overall response is similar to that of quartz grains embedded in a baked-clay tablet. Observing a ratio of 1.12 between the soil dose rate measured by $CaSO_4$–Dy in a polyethylene capsule and that measured when the capsule is inside the steel tube, he suggested that the low-energy region may carry about 4% of the total exposure. We see from Fig. 1 that overresponse is likely to be more serious with CaF_2 than with $CaSO_4$.

The wall material can modify response in two ways. First, there is selective attenuation of the spectrum, as just mentioned. Second, the TL phosphor may receive a significant dosage from the secondary electrons generated in the wall, depending on the relative absorption characteristics and the ranges of the electrons in the two media.

When relating observed dose rates to the energy-release predictions of Table 1, in addition to the relative response of the dosimeter material with respect to quartz, there is also the question of the absorption characteristics of the matrix—concrete in our experiments, soil or rock in the actual archaeological application. For dating, we used 100 μm quartz grains that received their dosage when embedded in a baked-clay matrix 1 or 2 cm across which, in turn, was surrounded by soil or rock. For the moment we are assuming that the absorption characteristics of quartz, soil, and rock are not significantly different. The small size of the quartz grains is also relevant here.

Some types of obsidian are much more TL sensitive than quartz, and, since obsidian is predominantly SiO_2, it can be used as a substitute for quartz. Assuming a typical obsidian composition of 10% Al_2O_3 and 84% SiO_2, with the remainder Na, K, and Ca (Taylor, 1977), we calculated absorption characteristics on the same basis as the other materials shown in Fig. 1. They were found to be indistinguishable from quartz between 50 keV and 3 MeV. Obsidian from a particular source in British Columbia (Obsidian Creek) was used because of its exceptional sensitivity; it permitted dose measurement down to 750 mrads at an uncertainty level of 3%, making it possible to work with a 9-day exposure in U3.

Lithium fluoride (Harshaw TLD-100) was also used; its rads-per-roentgen value is effectively constant in the energy region mentioned. This value is about 0.92 times that of concrete at high energies, falling to 0.2 at 50 keV. Thus LiF, if appropriately encapsulated in a material of similar average atomic number, can be expected to give a lower limit to the true infinite-matrix dose rate ("true" meaning the dose rate to the matrix itself).

The three phosphors were variously exposed in nylon, glass, aluminum, and copper, with wall thicknesses sufficient for effective removal of any beta contribution. An aluminum thickness of 1.5 mm was calculated to attenuate the total beta flux from the ^{238}U series by 97% (Evans, 1968a). The other walls are all more effective than this.

The observed dose rates at the center of U3 are given in Table 4. We can see that the obsidian-in-glass result is very near the matrix dose rate of 31.4 ± 0.8 rads/year derived from the concentration measurements.

In drawing conclusions from these data, it is useful to consider the attenuation caused by various types of capsule walls. Table 5 gives the value of $\exp(-\mu t)$ for various wall materials, where μ is the linear absorption coefficient (derived from Evans, 1968b) and t is the wall thickness.

TABLE 4

Observed Dose Rates (rads/year) in Block U3 with Various Dosimeter Materials*

Wall material and thickness	Natural CaF_2	Obsidian	LiF
Nylon, 4 mm	34.7 ± 0.3		30.7 ± 0.7
Glass, 3 mm		31.1 ± 0.9	
Aluminum, 1.5 mm	31.8 ± 0.1		
Copper, 0.7 mm	29.5 ± 0.1	40.0 ± 0.3	36.8 ± 0.8
	29.0 ± 0.2	38.7 ± 0.6	
	29.5 ± 0.3		

*Errors shown are standard errors on at least four measurements from each capsule.

TABLE 5

Effective Attenuation by Various Wall Materials*

Energy, MeV	Nylon, 4 mm	Glass, 3 mm	Aluminum, 1.5 mm	Copper, 1.5 mm
0.05	0.99	0.91	0.93	0.05
0.10	0.99	0.98	0.98	0.67
0.3	0.99	0.98	0.99	0.95
1.0	0.99	0.98	0.99	0.97
3.0	0.99	0.98	0.99	0.97

*The values are exp $(-\mu t)$, where μ is the linear absorption coefficient and t is the wall thickness (see discussion in text).

As mentioned earlier, LiF should absorb at least 8% less energy than a "concrete" dosimeter. Thus the LiF-in-nylon result (Table 4) defines a lower limit for the dose rate in concrete of 30.7 x 1.09 = 33.5 rads/year, including a 1% correction for wall attenuation.

Similarly, the CaF_2-in-nylon result can be used to define an upper limit. In the high-energy region, CaF_2 underresponds by 2% compared with concrete; including the low-energy region can only reduce this figure. Thus the dose rate in concrete must be less than 34.7 x 1.03 = 35.7 rads/year. We, therefore, took 34.6 ± 1.5 rads/year as the best estimate of the dose rate to concrete. This is about 10% more than the predicted dose rate of 31.4 ± 0.8 rads/year; this implies that the measured uranium concentration is too low—

leaving aside the possibility that Bell's downward revision of his dose-rate data was incorrect. The discrepancy is barely outside experimental error, however. Also, the predicted dose rate assumes a rather arbitrary 4% escape of radon, and perhaps the actual escape was less.

Following an argument similar to that in the preceding paragraphs, we expect the obsidian dose rate to be slightly less than 3% below the concrete dose rate (including the 2% glass capsule attenuation). In fact, this is within the measurement error.

Although calcium fluoride in aluminum gives the best match to the quartz dose rate, as recorded by obsidian in the glass capsule, it is not good practice to use aluminum routinely because of its significant level of radioactive impurity. Despite the need for a correction factor of 1.06, we prefer to use a copper capsule. In addition to the convenience of "near site" annealing, the activity in copper is negligible, and it is more resistant to corrosion. The correction factor will be a little smaller for the thorium and potassium spectra because of their smaller low-energy contribution; this is in the process of evaluation.

DIRECT MEASUREMENT OF GAMMA DOSE RATES WITH A NaI(Tl) DETECTOR

A NaI(Tl) crystal is a suitable detector for making an estimate of the intensity of a low-activity gamma flux. Converting this to a measure of energy absorbed by another medium (in this case CaF_2) independent of the energy of the gamma ray, however, requires that the ratio of the detection efficiency of NaI(Tl) to the mass absorption coefficient of CaF_2 be constant over the energy range of interest. As we see from Fig. 2, there is a gross overresponse of NaI with respect to CaF_2 below ~0.3 MeV; above this the response is virtually flat. There is a further effect caused by the relative sizes of the NaI detector and the phosphor used (typically 50 mg). The relative response shown in Fig. 2 is valid only if the mean free path through the detector and the phosphor are the same. As the NaI crystal size increases, the relative efficiency of detection of low-energy gammas decreases, compared with that of high-energy gammas, because the low energies are effectively stopped by the crystal. Thus there is a maximum size beyond which there can be no further increase in detection efficiency.

Unfortunately we are not dealing with a spectrum from a single parent. There are at least three independent contributors to the total gamma spectrum, the uranium and thorium chains and ^{40}K. Only if

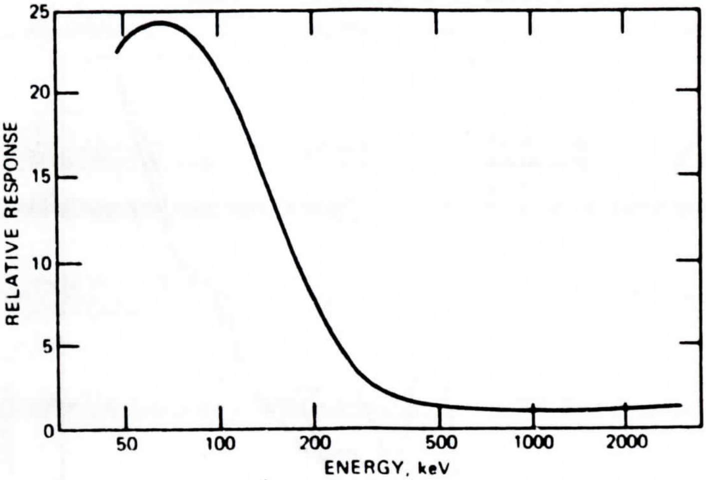

Fig. 2 Ratio of mass absorption characteristics of NaI to CaF_2. (See Fig. 1 for details of calculations.)

each of these deliver a similar proportion of energy to CaF_2 from the energy region of interest, as compared with the total energy delivered by the complete spectrum, will there be a single conversion ratio applicable to all three and independent of relative concentrations. At first glance this seems unlikely, especially since there is no low-energy contribution from ^{40}K; all absorbed low-energy gammas in the potassium spectrum are derived from Compton scattering in the medium and in the detector. In practice this absence is not important, however, as will be shown.

Experimental Procedures

The instrument used for our measurements was developed for the purpose. It consists of a NaI(Tl) crystal 1.75 in. in diameter and 2 in. high, with a photomultiplier tube (Centronic type P4231BA) in a watertight tubular aluminum housing connected to a self-contained high voltage generator and amplifier—discriminator with a scalar—timer. The instrument is powered by nickel—cadmium rechargeable batteries and weighs 4.5 kg to allow for field use. Gain stability is assisted by spectrum stabilization, with an ^{241}Am source mounted next to the detector in the aluminum housing. This source is held against the end of the crystal by a lead—cadmium—copper laminate designed to reduce the intensity of the low-energy gammas, which would otherwise interfere with the 60-keV stabilizing peak. This is important because it will further reduce the overresponse of

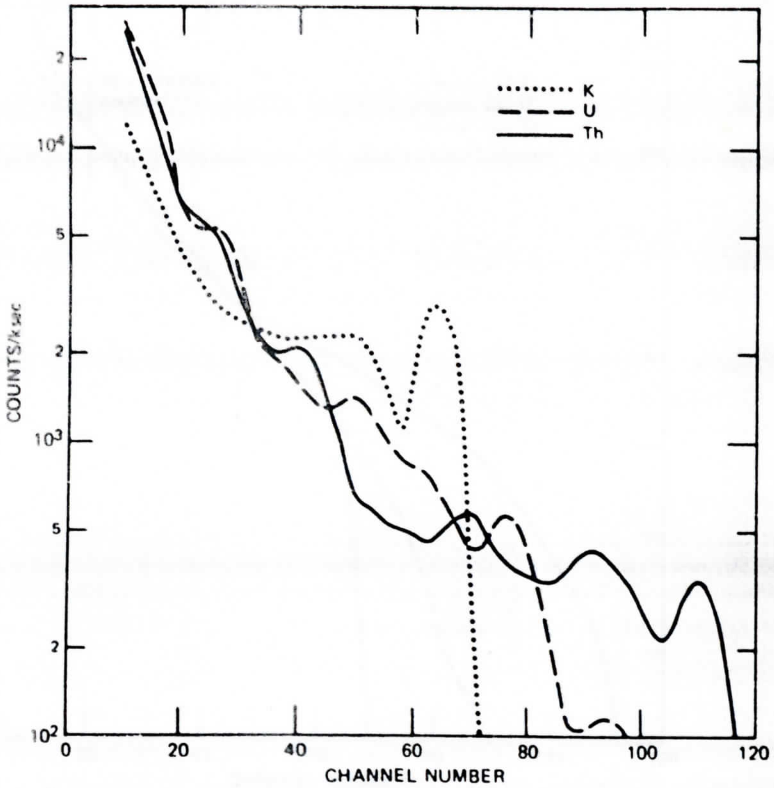

Fig. 3 **Block spectra, normalized to a dose rate of 1 mrad/day in CaF_2 and a count time of 1 ksec.**

the NaI crystal compared with CaF_2. A pulse-height analyzer was also used to obtain spectral information.

As a calibration facility we have available the four 51-cm concrete matrixes discussed earlier. We assume that they are sufficiently large to give a good approximation to the appropriate infinite-matrix spectral shape at the centers.

To determine the position of a suitable threshold, we recorded the gamma spectra above 0.1 MeV, using the pulse-height analyzer. These were then normalized to unit time, and the background spectrum was subtracted. The resulting spectra were divided by the appropriate dose rate (Table 3, item 4) to produce spectra seen by the NaI(Tl) crystal in 1 ksec, corresponding to a CaF_2 dose rate of 1 mrad/day. These are shown in Fig. 3. To determine the position of a suitable threshold, we then plotted the total counts recorded above a given energy in 1 ksec against energy as shown in Fig. 4.

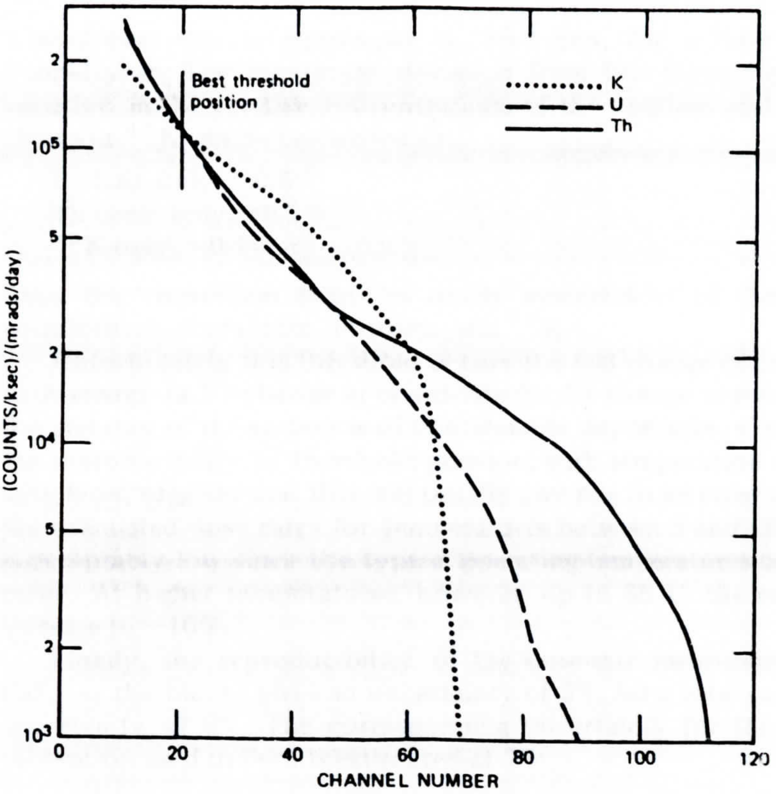

Fig. 4 Integral block spectra (calculated from Fig. 3).

Calibration and Errors

The original calibration used in the Peruvian results presented in the next section was at a threshold of about 0.6 MeV. The average count rate, assuming equal contributions from the uranium and thorium chains and from ^{40}K, was 12.9 cpm, for a dose rate in calcium fluoride of 1 mrad/year. If the site being measured was abnormally high in the concentration of any individual parent, the maximum error was calculated as:

U chain only, +0.05%
Th chain only, −5.5%
^{40}K only, +5.5%

The calibration from Fig. 4 suggests a revised threshold position at channel 20, corresponding to an energy of 0.45 MeV. This position gives an average count of 117 cps, for a dose rate in CaF_2 of

1 mrad/day; this is equivalent to 19.2 cpm, for a dose rate of 1 mrad/year. The maximum deviation from this figure because of variation in the relative concentrations of the uranium and thorium chains or ^{40}K can be calculated as:

U chain only, −0.5%
Th chain only, +0.7%
^{40}K only, −0.1%

Thus the conversion figure is nearly independent of the relative contribution of uranium, thorium, and ^{40}K.

Unfortunately this threshold occurs at a fast change of count rate with energy (a 1% change in count rate for 1% change in gain); hence the stability of the system is of considerable importance. Considering the reproducibility of threshold position, with temperature and after switch-on, suggests that this will usually give rise to an error of 3% on the calculated dose rates for temperatures between 5 and 20°C. This is acceptably low since the typical operating temperatures are in this range. At higher temperatures, however, up to 35°C, the error may increase to −10%.

Finally, the reproducibility of the dose-rate measurements for CaF_2 in the blocks gives an uncertainty of 5%, for a total calibration uncertainty of 6%. The corresponding uncertainty for the original calibration used in Peru is estimated at 7%.

Cosmic Contribution to Dose Rate

In the preceding discussion we assumed that the cosmic contribution had been removed from both the dose-rate measurements and the spectral measurements by subtracting the total background obtained from the background block. When counting on site, however, there will be some count rate from cosmic rays. This was estimated by submerging the detector in water with at least 1.5 m between the detector and the ground in all directions; this is sufficient to shield it from terrestrial radiation. The count rate observed, 65 cpm, is made up of a contribution from cosmic radiation, the activity in the crystal itself, and the activity in the photomultiplier tube.

The cosmic dose rate at a depth of about 50 cm in chalk was estimated by TL measurements to be 15 ± 0.15 mrads/year at sea level in Britain (latitude 51° N) by Aitken (1968). This depth corresponds to the likely burial depth of the detector on site. The count rate of 65 cpm will be observed when making site measurements near this latitude and altitude, whether it is of cosmic or scintillator origin. It must be subtracted from the observed count rate, and the cosmic dose-rate correction of 15 mrads/year is added on. Typically this is ~10% of the total dose rate.

It is interesting to note that Løvborg and Kirkegaard (1974) adopted a similar approach in calibrating a 3- by 3-in. crystal to determine the surface dose rate in air above geological formations with a threshold value of 0.37 MeV.

FIELD COMPARISON OF SCINTILLATOR AND CAPSULE MEASUREMENTS ON PERUVIAN ARCHAEOLOGICAL SITES

Some 46 different sites were visited between June and September 1975; half were near sea level (at altitudes less than 250 m), and half were at altitudes between 3000 and 4500 m. At all sites several measurements of the dose rates were made at a depth of not less than 30 cm in soil (usually about 50 cm), with both a 1.75-in.-diameter by 2-in. and a 1-in.-diameter by 2-in. crystal. At 19 of the sites, it was possible to bury capsules for eventual recovery, usually in the borehole made for the detector. Both crystals were calibrated as previously discussed, and the results agree well. Further discussion is restricted to the results from the 1.75-in.-diameter detector.

All the coastal sites were dry (water contents were less than 10% of dry weight). Some of the highland sites were very wet (water contents were 60% of dry weight).

Capsule Dose Rates

Although it was possible to anneal the capsules a few hours before burial, readout was a minimum of 10 days after recovery—in some cases 50 days. This included an air flight of 18 hr. During this time the capsules were stored in lead pots with 0.25-in. wall thicknesses, selected for low radioactive contamination. Since the maximum burial time was 72 days, it is obviously important to make an accurate estimate of the "carriage" dose rate; i.e., the dose rate from terrestrial and cosmic radiation and internal activity of the CaF_2 (termed "self dose") while the capsule was being returned to the laboratory. This was done by retaining one capsule from every batch annealed for burial and storing this directly in the lead pots so that the capsules would record only the carriage dose. These dose rates are listed in Table 6.

Since the spread in the average dose rate is unusually large if all the capsules are indeed measuring the same quantity, it was decided to assess two distinct dose rates, one at sea level and one in the

TABLE 6

Carriage Dose Rates Recorded by CaF_2 in Copper in 0.25-in. Lead Pots

Capsule number	Recorded dose, mrads	Days at sea level	Days in highlands	Dose rate, mrads/year
III	25.4	57	40	96
VIII	23.6	47	40	99
XII	23.5	39	40	109
XVIII	19.4	31	38	103
LXVI	14.5	51	9	88
XXIII	33.3	43	66	112
LVIII	24.2	17	58	118
			Average	104
			Sigma	10%

Linear regression analysis, assuming two distinct dose rates:

Sea-level dose rate	Highland dose rate
76.3 mrads/year	130.7 mrads/year
Sigma 6%	Sigma 3%

highlands. Two rates could be expected because of the higher level of cosmic radiation at higher altitudes.

The better fit of the results obtained by least-squares regression on the data (Table 6) confirms that there are in fact two distinct dose rates. Using these figures, we calculated the site dose rates listed in Table 7. A self dose in CaF_2 of 11 mrads/year, which had been previously assessed for the type of CaF_2 used (Aitken, 1968), was assumed during burial. During transport this is included in the carriage dose rate.

Scintillator Dose Rates

Before comparing scintillator and capsule results directly, further thought must be given to the cosmic-ray correction for two reasons, latitude and altitude effects.

Latitude Effect

Peru is at a latitude of 12° S; Oxford is about 51.5° N. Assuming the cosmic dose at a depth of 50 cm to be from only the hard component, the intensity at sea level in Peru is likely to be about 0.91 of that at sea level in the United Kingdom (NCRP, 1976); i.e., a

TABLE 7

CaF$_2$ and Scintillator Dose Rates

Site number	Water, %	Total dose, mrads,	Burial time, days	Carriage		Dose rate, mrads/year	Scintillator dose rate (+ corrections), mrads/year	
				Sea level, days	Highland, days		cosmic	water (%)
				Sea-Level Sites				
P02K	1.6	41.9	70	16	0	190	155	147
P04J	4.6	28.1	72	14	0	117	128	125
P06N	8.7	31.2	71	14	0	135	151	153
P10K	3.2	32.0	68	15	0	144	138	133
P12Q	8.1	25.8	67	14	0	113	121	122
P17L	1.8	24.3	62	17	0	111	129	123
P23	1.9	28.1	59	17	0	141	151	143
P34	3.1	20.9	51	17	0	113	120	115
P35I/J	0.6	28.5	54	14	0	162	152	143
P35K	0.6	22.8	54	12	0	126	137	129
P36A	1.2	16.0	53	14	0	78	97	91
				Highland Sites				
P37J	25	35.4	60	42	6	139	109	126
P37L	24	37.6.	60	42	6	152	120	137
P37Q$_1$	30	28.5	60	42	6	97	87	103
P37Q$_2$	30	39.2	60	42	6	161	114	133
P39J	36	37.9	58	42	4	162	121	151
P40	63	26.7	58	42	4	93	71	112
P44$_1$	12	64.5	51	18	26	358	211	219
P44$_2$	12	47.2	51	18	26	234	211	219
P44$_3$	12	47.4	51	18	26	235	211	219
P45	11	34.0	56	18	21	137	104	107
P46J$_1$		48.9	51	17	7	296	187	
P46J$_2$		36.9	51	17	7	210	187	

dose rate of about 13 ± 2 mrads/year. The scintillator count rate when surrounded by 1.5 m of water was measured near sea level in Peru as 65 ± 3 cpm; this was subtracted from the observed-site count rates before converting to dose rates. The cosmic dose rate of 13 mrads/year was then added to give the total dose rate determined by the scintillator.

Altitude Effect

At an altitude of 4 km the intensity of the hard component will be between two and three times that at sea level (Lowder, 1978; derived from data in NCRP, 1975; O'Brien, 1975). At a level of 30 ± 4 mrads/year, this provides an important fraction of the total dose rate and must be added to the dose rate predicted by the scintillator count rate obtained after subtracting the count rate submerged in water, which was measured at an altitude of 3.5 km as 121 ± 5 cpm.

It is interesting to note that, if the increase in count rate when submerged in water is attributed solely to the increase by a factor of 2.3 in the cosmic-ray intensity, a "true" sea-level cosmic count rate of 24 cpm is predicted. Thus it seems likely that impurities in the detector head contribute about 40 cpm.

Capsule and scintillator results are listed in columns 7 and 8 of Table 7, with the appropriate cosmic correction included in the scintillator data.

We suggest that the results from sites $P44_1$, $P46J_1$, and $P46J_2$ be disregarded. The $P44_1$ result is not consistent with $P44_2$ and $P44_3$. Since all three capsules were in the same borehole, this suggests a local inhomogeneity to which the capsule would be much more sensitive than the scintillator. Site P46 was very poor f · n the point of view of dosimetry; the detector and capsules were placed at the boundary of a soil layer with loose slate and vegetation.

A brief examination of the cosmic-corrected scintillator and capsule results shows that, although the lowland sites give moderate agreement, the scintillator gives consistently low readings compared with the capsules in the highland sites. Assuming the amount added for the cosmic contribution at a high altitude to be correct (it would need to be doubled to remove the discrepancy), a possible reason for the difference is the change in radon retention when the soil is disturbed to insert the scintillator and capsule—especially on wet sites. It is well known that water plays an important part in radon emanation and transport (see, e.g., Tanner, 1964). Most of the gamma dose rate and scintillator count rate from the uranium chain is derived from radon daughters, and the scintillator measures the count rate from these daughters with the soil in a recently disturbed state, partially dried out after excavation. The capsule is buried, however, and measures the dose rate with the surrounding soil close to its original condition over a long period of time compared with the radon half-life. Although this change in emanation is likely to be variable, some correlation between water content and the fractional difference of the capsule and scintillator dose rates can be seen.

The last column in Table 7 lists the scintillator results after a water-content correction is applied:

$$\begin{array}{c}\text{Corrected}\\ \text{scintillator}\\ \text{dose rate}\end{array} = \begin{array}{c}\text{Scintillator}\\ \text{dose rate}\end{array} \times \left[1 + \frac{1}{100}(0.85 \times W - 6.4)\right]$$

where W is the percentage water content of the soil. This equation was empirically derived from the capsule and cosmic-corrected scintillator data in Table 7. (Of course, such a water-content correction should be applied only to the portion of the gamma dose that is derived from radon daughters). It is worth noting that the intercept term, implying that no correction is necessary if the water content is ~7.5%, is consistent with the measured water content of the calibration blocks, ~8%.

This correction formula almost completely removed the systematic difference in the highland results (less than 5 ± 5% to one sigma) and further reduced any average difference in the sea-level data (less than 2 ± 4% to one sigma), without increasing the spread of the differences, ~12% to one sigma.

This comparison of capsule and scintillator results cannot be considered conclusive because of the relatively large corrections to both sets of results. For those sites where it was impossible to use a capsule, however, it does show that the measurements taken with the scintillator are meaningful if the appropriate cosmic and water-content corrections are applied.

ACKNOWLEDGMENTS

We are grateful to D. A. Morris for designing the spectrum stabilization for the scintillator; to M. Marshall, United Kingdom Atomic Energy Research Establishment, Harwell, for gamma spectrometry of the U. S. Department of Energy ore; and to Erle Nelson, Simon Fraser University, for providing the obsidian.

S. G. E. Bowman and A. S. Murray gratefully acknowledge financial support from Natural Environment Research Council

(NERC) studentships. The Peruvian data came from work undertaken by the Oxford and Liverpool Universities Archaeomagnetic Expedition 1975, also financed by the NERC.

Finally, we are indebted to Wayne M. Lowder for his helpful comments and advice.

REFERENCES

Aitken, M. J., 1968, Low-Level Environmental Radiation Measurements Using Natural Calcium Fluoride, in *Proceedings of the Second International Conference on Luminescence Dosimetry*, Gatlinburg, Tenn., Sept. 23—26, 1968, J. A. Auxier, K. Becker, and E. M. Robinson (Eds.), USAEC Report CONF-680920, pp. 281-290, Oak Ridge National Laboratory, NTIS.

——, 1975, *Physics and Archaeology*, 2nd Ed., Chap. 3, Clarendon Press, Oxford University.

——, and S. J. Fleming, 1972, Thermoluminescence Dosimetry in Archaeological Dating, in *Radiation Dosimetry*, Supplement 1, *Topics in Radiation Dosimetry*, F. H. Attix and W. Roesch (Eds.), Academic Press, Inc., New York.

——, D. W. Zimmerman, and S. J. Fleming, 1968, Thermoluminescent Dating of Ancient Pottery, *Nature*, 219: 442-444.

Bell, W. T., 1976, The Assessment of the Radiation Dose Rate for Thermoluminescence Dating, *Archaeometry*, 18(1): 107-111.

——, 1977, Thermoluminescent Dating: Revision of Dose Rate Data, *Archaeometry*, 19(1): 100.

Bowman, S. G. E., 1976, Ph.D. Thesis, App. A5, Oxford University, Oxford, England.

Evans, R. D., 1968a, *The Atomic Nucleus*, p. 627, McGraw-Hill Book Company, London.

——, 1968b, X-Ray and Gamma Interactions, in *Radiation Dosimetry*, Vol. 1, *Fundamentals*, 2nd ed., F. H. Attix and W. C. Roesch (Eds.), pp. 94-144, Academic Press, Inc., New York.

Fleming, S. J., 1977, *Dating in Archaeology*, Chap. 5, J. M. Dent & Sons, Ltd., London.

Løvborg, L., and P. Kirkegaard, 1974, Response of 3″ × 3″ NaI(Tl) Detectors to Terrestrial Gamma Radiation, *Nucl. Instrum. Methods*, 121: 239-251.

Lowder, W. M., 1978, U. S. Department of Energy, Environmental Measurements Laboratory, New York, personal communication.

Mejdahl, V., 1970, Measurement of Environmental Radiation at Archaeological Excavation Sites, *Archaeometry*, 12(2): 147-159.

——, 1972, *Dosimetry Technique in Thermoluminescent Dating*, Risø Report No. 261, Research Establishment Risø, Danish Atomic Energy Commission.

NCRP, 1975, *Natural Background Radiation in the United States*, NCRP Report 45, p. 12, National Council on Radiation Protection and Measurements, Washington, D. C.

——, 1976, *Environmental Radiation Measurements*, NCRP Report 50, p. 31, National Council on Radiation Protection and Measurements, Washington, D. C.

O'Brien, K., 1975, The Cosmic Ray Field at Ground Level, in *The Natural Radiation Environment II*, Symposium Proceedings, Houston, Tex., Aug. 7—11, 1972, J. A. S. Adams, W. M. Lowder, and T. F. Gesell (Eds.), ERDA Report CONF-720805, Rice University and the University of Texas, Houston, NTIS.

Storm, E., and H. I. Israel, 1970, *Nuclear Data Tables, A7*, p. 565, Academic Press, Inc., New York.

Tanner, A. B., 1964, Radon Migration in the Ground-A Review, in *The Natural Radiation Environment*, J. A. S. Adams and W. M. Lowder (Eds.), University of Chicago Press, Chicago.

Taylor, R. E. (Ed.), 1977, Advances in Obsidian Glass Studies: Archaeological and Geochemical Perspectives, Noyes Data Corp., Park Ridge, N. J.

Warren, S. E., 1978, Rubidium—A Potential Source of Systematic Error in Thermoluminescence Dating of Pottery, *Archaeometry*, 20: 66-70.

Wintle, A. G., 1973, Anomalous Fading of Thermoluminescence in Mineral Samples, *Nature*, 245: 143-144.

——, and A. S. Murray, 1977, Thermoluminescence Dating: Reassessment of the Fine Grain Dose Rate, *Archaeometry*, 19(1): 97.

Zimmerman, D. W., 1971, Thermoluminescent Dating Using Fine Grains from Pottery, *Archaeometry*, 13(1): 29-52.

——, 1972, Relative Thermoluminescence Effects of Alpha and Beta Radiation, *Radiat. Eff.*, 14: 81-92.